SCIENCE CHINA
Information Sciences

• RESEARCH PAPER •

September 2016, Vol. 59 092210:1–092210:19
doi: 10.1007/s11432-015-5384-9

Predictor-based neural dynamic surface control for distributed formation tracking of multiple marine surface vehicles with improved transient performance

Zhouhua PENG[1,2*], Dan WANG[1] & Tieshan LI[3]

[1]*School of Marine Engineering, Dalian Maritime University, Dalian* 116026*, China;*
[2]*Control Science and Engineering, Dalian University of Technology, Dalian* 116024*, China;*
[3]*School of Navigation, Dalian Maritime University, Dalian* 116026*, China*

Received January 16, 2016; accepted April 15, 2016; published online August 23, 2016

Abstract In this paper, we investigate the distributed formation tracking problem of multiple marine surface vehicles with model uncertainty and time-varying ocean disturbances induced by wind, waves, and ocean currents. The objective is to achieve a collective tracking with a time-varying trajectory, which can only be accessed by a fraction of follower vehicles. A novel predictor-based neural dynamic surface control design approach is proposed to develop the distributed adaptive formation controllers. We use prediction errors, rather than tracking errors, to construct the neural adaptive laws, which enable the fast identification of the vehicle dynamics without incurring high-frequency oscillations in control signals. We establish the stability properties of the closed-loop network via Lyapunov analysis, and quantify the transient performance by deriving the truncated L_2 norms of the derivatives of neural weights, which we demonstrate to be smaller than the classical neural dynamic surface control design approach. We also extend the above result to the distributed formation tracking using the relative position information of vehicles, and the advantage is that the velocity information of neighbors and leader are required. Finally, we give the comparative studies to illustrate the performance improvement of the proposed method.

Keywords dynamic surface control, distributed formation tracking, predictor, marine surface vehicles, neural networks

Citation Peng Z H, Wang D, Li T S. Predictor-based neural dynamic surface control for distributed formation tracking of multiple marine surface vehicles with improved transient performance. Sci China Inf Sci, 2016, 59(9): 092210, doi: 10.1007/s11432-015-5384-9

1 Introduction

In recent years, there has been a surge of interest in cooperative control of multi-vehicle systems. Applications can be found everywhere; in space, air, land, and sea. Examples include formation flying of spacecrafts and aircrafts, formation control of mobile robots, and fleet control of marine vehicles, including surface vehicles and underwater vehicles. Apparently, multi-vehicle systems enable individuals to

* Corresponding author (email: zhouhuapeng@gmail.com)

collaborate with each other to execute difficult missions, offering greater advantage over a single one in the sense of enhanced effectiveness and efficiency [1, 2].

Formation control of marine vehicles has drawn great attention from control communities. In the literature, a variety of approaches to this problem have been reported [3–11]. In general, these approaches fall into three categories, namely, virtual structure, behavioral approach, and leader-follower strategy. Most works are practiced within the leader-follower framework [3–10]. In [3], a coordinated path following scheme is proposed to solve the geometric task and dynamic task in a rigid leader-follower formation. In [4], a passivity-based design is presented for synchronized path following where the path variables are coordinated in a decentralized manner. A similar coordinated path following solution can be found in [5]. In general, this approach is able to achieve rigid formations if a predefined path is assigned to each vehicle. However, once the mission changes or something unexpected happens, the original paths must be redesigned for the new situation. In [6], a guided leader-follower formation control scheme is presented, where no path information is known as a priori. In [7], a leader-follower synchronization approach without velocity information is proposed. In [8], a virtual leader-based formation control scheme is proposed for underactuated underwater vehicles. In [9, 10], $l - \psi$ leader-follower formation controllers are developed for autonomous surface vehicles where the uncertain vehicle dynamics is taken into account. In the aforementioned studies, the formation control objective can be achieved if each vehicle is able to obtain the leader information in global coordinates. However, the leader information may not be known to all vehicles due to the limitations of communication bandwidth and sensing range. Besides, it will be costly to convey the leader information to each vehicle. This situation worsens when a large number of vehicles are involved.

In fact, distributed control strategy has been widely suggested for multi-agent systems; see references [12–15]. Its key advantage is that the global objective can be achieved via neighbor-to-neighbor information exchange, which is closely related to consensus problem [16–32]. Different from traditional tracking control of a single system, the main challenge is to seek local policies such that the final states of all agents can reach an agreement. Today, as consensus theory evolves, studies have been devoted to its applications in real-world agents, such as spacecrafts [33], mobile robots [34], and autonomous underwater vehicles [35]. From the standpoint of marine engineering, it will be interesting to apply consensus theory to address the formation control of marine surface vehicles (MSVs).

On the other hand, since the dynamics of MSV belongs to a class of nonlinear systems in strict-feedback form [36], the backstepping technique has been a powerful design tool to develop the tracking controllers [37–42] and the formation controllers [3–5,8,9]. A disadvantage with backstepping is the problem of "explosion of complexity", which is caused by the repeated differentiations of virtual control signals. In [43], a dynamic surface control (DSC) design technique was proposed to avoid the repeated differentiation problem of virtual controllers in the backstepping design. The key is introducing a first-order filtering of the synthesized virtual control law at each step of the backstepping design procedure. In [44], a neural DSC (NDSC) design approach is first proposed for tracking of uncertain nonlinear strict-feedback systems. From then on, substantial efforts have been devoted to neural network-based DSC design for nonlinear systems [44–51].

However, the traditional NDSC approach suffers from poor transient performance phenomenon, which can be speculated as follows: First, the system states can be far different from the filtered virtual control signals during transient (i.e., in the initial stage or transitions between different equilibrium points). It may deteriorate the NN learning process and experience the control signals of large-amplitude, which are unacceptable for practical applications. Second, high-gain learning rates are often required to achieve system performance in the face of large uncertainties. However, updating laws with high learning rates may yield signals of high-frequency, which can, for example, excite unmodeled dynamics, and even result in instability for real-world applications. There have been great efforts on modifications of control architectures or updating laws for improving the transient performance of adaptive control systems [52–54]. However, most works are practiced within the model reference adaptive control framework. Up until now, it seems that no attempt has been made to improve the transient performance of neural DSC approach, although it shows potential usage in many real-world applications.

In this paper, we focuses on the distributed formation tracking (DFT) of multiple MSVs, each of which is governed by nonlinear dynamics with model uncertainty and unknown ocean disturbances induced by wind, waves, and ocean currents. The objective is to achieve a collective tracking with a time-varying trajectory that can be accessed by a fraction of the follower vehicles. We define a new type of predictor-based neural dynamic surface control (PNDSC) design method by combining a predictor, neural networks (NNs), and a DSC design approach, with which the control performance can be substantially improved. A predictor is, for the first time, introduced in the traditional NN-based DSC design. The prediction errors, rather than the tracking errors, are employed to update the NN parameters, which enable smooth and fast learning without incurring high-frequency oscillations. With this new design approach, robust adaptive DFT controllers are developed for directed graphs containing a spanning tree. The stability properties of the closed-loop systems are established building on Lyapunov theory and graph theory. In addition, we qualify the transient performance of the proposed PNDSC architecture in terms of truncated L_2 norms of the derivatives of neural weights, which are shown to be smaller than the classical NDSC design approach by rigorous analysis. An extension to DFT using the relative position information of vehicles is further studied; i.e., the velocity information of leader and neighbors are all not required for implementation. Comparative studies are given to illustrate the performance improvement of the proposed approach.

Compared with existing results, the contribution of this paper is three-fold.

• First, in contrast to the NN-based DSC approach [44–51], a new type of PNDSC design methodology, by combining a predictor, NNs, and a DSC technique, is proposed. The predictor is first introduced into the NN-based DSC design. The prediction errors are employed to identify the unknown dynamics for each vehicle, and an additional adjustable parameter is provided to enable smooth and fast learning not only in steady state, but also in transient state. The undesired learning transient when using NDSC approach due to large initial tracking errors can be completely avoided. In this regard, the proposed design methodology is an enhanced version of NDSC approach proposed for nonlinear systems in Ref. [44], with guaranteed steady and transient performance. To the best of our knowledge, it is the first attempt to address the transient performance of NN-based DSC design as apposed to Refs. [44–51].

• Second, this paper aims to address the DFT control of multiple MSVs with a dynamic leader over directed graphs because of the lack of global information on the reference trajectory; i.e., only a fraction of follower MSVs can receive the information of the leader. This is different from the tracking control of single MSV in [37–41] and the leader-follower formation control of multiple MSVs in [3–10], where the leader or path information is known to each vehicle. Inherently, this work was inspired by formation control of multi-agent systems with first-order and second-order dynamics. However, the dynamics of MSVs cannot be described by first-order and second-order dynamics because two reference frames are commonly used for marine vehicles. By defining a distributed formation tracking error expressed in body-fixed reference frame, the DFT problem can be readily solved without incurring complexity. This also does not seem to have been reported in the marine literature.

• Third, robust adaptive DFT controllers are developed based on the new PNDSC approach, and an extension to DFT using the relative position information is further studied. Note that the velocity information of leader and neighbors can be recovered on-line by the proposed predictors for the second case. This is practically useful in case only the local sensors (e.g. visual sensors) are equipped. It is worthwhile to mention that the traditional trajectory tracking of MSVs can be considered as a special case of the results derived in this paper.

The rest of this paper is organized as follows: Section 2 introduces some preliminaries and the problem formulation. Section 3 presents the DFT design together with the stability analysis. Section 4 extends the above result to DFT using relative position information. Section 5 provides simulation results to illustrate the theoretical results. Section 6 concludes this paper.

2 Preliminaries and problem formulation

2.1 Preliminaries

2.1.1 *Notation*

Throughout the paper, the n-dimensional Euclidean space is denoted by $\mathbb{R}^n$. I_n represents an identity matrix of dimension n. The superscript T means transpose for real matrices. $\mathrm{diag}\{a_i\}$ is a block-diagonal matrix with matrixes $a_i, i = 1, \ldots, N$, on its diagonal. For a square matrix, the eigenvalue, the smallest eigenvalue and the largest eigenvalue are denoted by $\lambda(\cdot)$, $\lambda_{\min}(\cdot)$, and $\lambda_{\max}(\cdot)$, respectively. $\|\cdot\|$ is the Euclidean norm for a given vector, and $\|\cdot\|_F$ is the Frobenius norm for a matrix. Given $p \geqslant 1$ and $v \in \mathbb{R}^n$, the L_p norm and truncated L_p norm is defined by $\|v\|_{L_p} = (\int_0^\infty \|v(s)\|^p \mathrm{d}s)^{1/p}$ and $\|v\|_{L_p,t^*} = (\int_0^{t^*} \|v(s)\|^p \mathrm{d}s)^{1/p}$ with $t^* > 0$, respectively.

2.1.2 *Graph theory*

A graph $\mathcal{G} = \{\mathcal{V}, \mathcal{E}\}$ consists of a node set $\mathcal{V} = \{n_1, \ldots, n_N\}$ and an edge set $\mathcal{E} = \{(n_i, n_j) \in \mathcal{V} \times \mathcal{V}\}$ with element (n_i, n_j) that describes the communication from node i to node j. An adjacency matrix is defined as $\mathcal{A} = [a_{ij}] \in \mathbb{R}^{N\times N}$ with $a_{ij} = 1$, if $(n_j, n_i) \in \mathcal{E}$; and $a_{ij} = 0$, otherwise. Self connections are not allowed, i.e., $a_{ii} = 0$. The Laplacian matrix $\mathcal{L}$ associated with the graph $\mathcal{G}$ is defined as $\mathcal{L} = \mathcal{D} - \mathcal{A}$ where $\mathcal{D} = \mathrm{diag}\{d_1, \ldots, d_N\}$ with $d_i = \sum_{j=1}^N a_{ij}$, $i = 1, \ldots, N$. A directed path in the graph is an ordered sequence of nodes such that any two consecutive nodes in the sequence are an edge of the graph. A digraph has a spanning tree if there is a node called the root, such that there is a directed path from the root to every other node in the graph. Finally, define a diagonal matrix $\mathcal{A}_0 = \mathrm{diag}\{a_{10}, \ldots, a_{N0}\}$ to be a leader adjacency matrix, where $a_{i0} > 0$ if and only if the ith vehicle has access to the information of the leader; otherwise $a_{i0} = 0$. For simplicity, let $\mathcal{H} = \mathcal{L} + \mathcal{A}_0$.

2.2 Problem formulation

To describe the motion of MSV, two reference frames, as shown in Figure 1, are commonly used, a earth-fixed frame and a body-fixed frame. A three degree-of-freedom (DOF) dynamic model for MSVs in a horizontal plane can be found in [55], and consists of kinematics

$$\dot{\eta}_i = R(\psi_i)\nu_i, \tag{1}$$

and kinetics

$$M_i\dot{\nu}_i = -C_i(\nu_i)\nu_i - D_i(\nu_i)\nu_i + \tau_i + R^{\mathrm{T}}(\psi_i)\tau_{iw}(t), \tag{2}$$

where

$$R(\psi_i) = \begin{bmatrix} \cos\psi_i & -\sin\psi_i & 0 \\ \sin\psi_i & \cos\psi_i & 0 \\ 0 & 0 & 1 \end{bmatrix}, \tag{3}$$

$\eta_i = [x_i, y_i, \psi_i]^{\mathrm{T}} \in \mathbb{R}^3$ represents the earth-fixed position and heading; $\nu_i = [u_i, v_i, r_i]^{\mathrm{T}} \in \mathbb{R}^3$ includes the body-fixed surge and sway velocities, and the yaw rate; $M_i = M_i^{\mathrm{T}} \in \mathbb{R}^{3\times3}, C_i(\nu_i) \in \mathbb{R}^{3\times3}, D_i(\nu_i) \in \mathbb{R}^{3\times3}$ denote the inertia matrix, coriolis/centripetal matrix, and damping matrix, respectively; $\tau_i = [\tau_{iu}, \tau_{iv}, \tau_{ir}]^{\mathrm{T}} \in \mathbb{R}^3$ denotes the control force; $\tau_{iw}(t) = [\tau_{iwu}(t), \tau_{iwv}(t), \tau_{iwr}(t)]^{\mathrm{T}} \in \mathbb{R}^3$ is the disturbance vector caused by unknown wind, waves, and ocean currents. In practice, $C_i(\nu_i)$, $D_i(\nu_i)$, and $\tau_{iw}(t)$ are very hard to model or measure accurately, and here, they are treated as completely unknown functions. Note that the value of M_i, $C_i(\nu_i)$, and $D_i(\nu_i)$ can be different; hence, the vehicles considered are heterogenous.

Consider a reference $\eta_0 \in \mathbb{R}^3$ that acts as a leader (labeled as n_0), and then the communication graph among the N vehicles and the reference trajectory η_0 can be described by an augmented graph

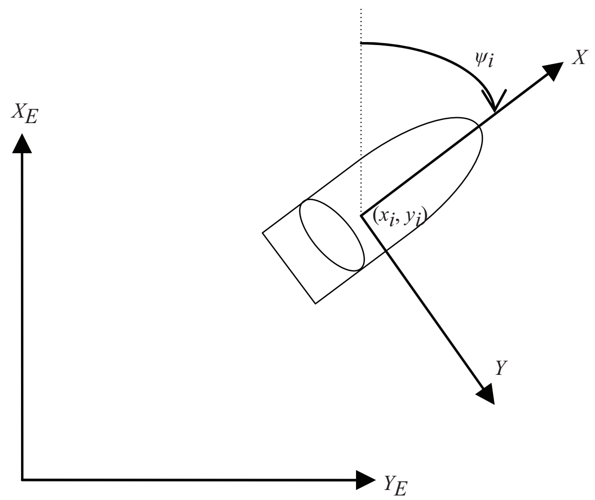

Figure 1 Reference frames: earth-fixed and body-fixed.

$\bar{\mathcal{G}} = \{\bar{\mathcal{V}}, \bar{\mathcal{E}}\}$ where $\bar{\mathcal{V}} = \{n_0, n_1, \ldots, n_N\}$, and $\bar{\mathcal{E}} = \{(n_i, n_j) \in \bar{\mathcal{V}} \times \bar{\mathcal{V}}\}$. To move on, the following assumption is required.

Assumption 1. The augmented graph $\bar{\mathcal{G}}$ contains a spanning tree with the root node being the leader node n_0.

Definition 1. A geometric pattern between the vehicles is defined in the earth-fixed frame as $\mathcal{P} = \{\mathcal{P}_i\}$ and $\mathcal{P}_i = [p_{ix}, p_{iy}, p_{i\psi}]^{\mathrm{T}}$ where $p_{ix}, p_{iy}, p_{i\psi}$ are constants. $\mathcal{P}_{ij} = \mathcal{P}_i - \mathcal{P}_j$ represents the desired relative deviation between the ith vehicle and jth vehicle.

Without lose of generality, we assume that $\sum_{i=1}^{N} \mathcal{P}_i = [0, 0, 0]^{\mathrm{T}}$, which means that the center of the geometric pattern $\mathcal{P}$ is at the origin.

Remark 1. Note that a common reference frame is needed to define the geometric pattern; however, this can be naturally satisfied for MSVs because they use global positioning systems (GPS) to acquire their positions [55]. Otherwise, one has to alteratively resort to distributed algorithms [56] to estimate the common reference frame.

The DFT problem is stated as below.

The control objective is to design a distributed control law τ_i for each vehicle with the kinematics (1) and kinetics (2) to track a reference signal η_0 with the desired geometric pattern $\mathcal{P}$ such that

$$\lim_{t\to\infty} \|\eta_i - \eta_j - \mathcal{P}_{ij}\| \leqslant \delta_1, i, j = 1, \ldots, N, \tag{4}$$

$$\lim_{t\to\infty} \left\| \sum_{i=1}^{N} \frac{\eta_i}{N} - \eta_0 \right\| \leqslant \delta_2, \tag{5}$$

for some constants δ_1 and δ_2.

Remark 2. Inequality (4) means that the MSVs achieve the geometric formation pattern $\mathcal{P}$ with bounded errors; while inequality (5) indicates that the geometric center of the MSVs converge to the reference η_0 with small errors.

3 DFT using neighbors' velocity information

In this section, we consider the case where the position and velocity information of neighboring vehicles are available for feedback. A new PNDSC design approach is proposed to devise the distributed formation controllers, under which a relative formation can be achieved for directed graphs containing a spanning tree.

3.1 Controller design

Step 1. To start with, a distributed surface tracking error z_{i1} is defined as follows:

$$z_{i1} = R^{\mathrm{T}}(\psi_i)\left\{\sum_{j=1}^{N} a_{ij}(\eta_i - \mathcal{P}_i - \eta_j + \mathcal{P}_j) + a_{i0}(\eta_i - \mathcal{P}_i - \eta_0)\right\}, \tag{6}$$

where a_{ij} and a_{i0} are defined in Section 2. η_j is the earth-fixed position and heading for jth vehicle. $\mathcal{P}_i$ is the deviation between the ith vehicle and the reference trajectory η_0. Whether the ith vehicle has access to the reference trajectory η_0 is determined by the network links.

Remark 3. Note that the surface tracking error z_{i1} is defined in the body-fixed reference frame, which makes the consensus theory well suitable for the applications of marine vehicles. This also means that the controller gains will not depend on the heading of the vehicle, as pointed out in [42]. Compared with diffeomorphic coordinate transformation $z = R^{\mathrm{T}}(\psi_i)(\eta_i - \eta_0)$ introduced for tracking control of single vehicle as in [39, 42], here, distributed diffeomorphic coordinate transformation is introduced to solve the coordinated control of multiple MSVs.

Further, a global formation tracking error s_i is defined as

$$s_i = \eta_i - \mathcal{P}_i - \eta_0. \tag{7}$$

Let $z_1 = [z_{11}^{\mathrm{T}}, \ldots, z_{N1}^{\mathrm{T}}]^{\mathrm{T}}$ and $s = [s_1^{\mathrm{T}}, \ldots, s_N^{\mathrm{T}}]^{\mathrm{T}}$ be the error vectors of the network, and their relationship can be expressed as

$$z_1 = \mathcal{R}^{\mathrm{T}}(\mathcal{H} \otimes I_3)s, \tag{8}$$

where $\mathcal{R} = \mathrm{diag}(R(\psi_1), \ldots, R(\psi_N))$, and $\mathcal{H}$ is defined in Section 2.

The following lemma holds for (8).

Lemma 1 [19, 27]. Under Assumption 1, $\|s\| \leqslant \|z_1\|/\underline{\varrho}(\mathcal{H})$ where $\underline{\varrho}(\mathcal{H})$ denotes the minimal singular value of $\mathcal{H}$.

The time derivative of z_{i1} with (1) is given by

$$\dot{z}_{i1} = -r_i S z_{i1} + a_{id}\nu_i - \sum_{j=1}^{N} a_{ij} R_i^{\mathrm{T}} R_j \nu_j - a_{i0} R_i^{\mathrm{T}} \dot{\eta}_0, \tag{9}$$

where $a_{id} = d_i + a_{i0}$, $R_i = R(\psi_i)$, $R_j = R(\psi_j)$, and S is defined by

$$S = \begin{bmatrix} 0 & -1 & 0 \\ 1 & 0 & 0 \\ 0 & 0 & 0 \end{bmatrix}. \tag{10}$$

In order to stabilize z_{i1}, a virtual kinematic law α_{i1} is proposed as follows:

$$\alpha_{i1} = \frac{1}{a_{id}}\left(-k_{i1}z_{i1} + \sum_{j=1}^{N} a_{ij} R_i^{\mathrm{T}} R_j \nu_j + a_{i0} R_i^{\mathrm{T}} \dot{\eta}_0\right), \tag{11}$$

where $k_{i1} = \mathrm{diag}\{k_{i11}, k_{i12}, k_{i13}\}$ with $k_{i11} \in \mathbb{R}$, $k_{i12} \in \mathbb{R}$, $k_{i13} \in \mathbb{R}$ being positive constants.

Let α_{i1} pass through a first-order filter bank with a time constant $\gamma_{i1} \in \mathbb{R}$ to obtain the filtered control signal ν_{ir} as follows:

$$\gamma_{i1}\dot{\nu}_{ir} = \alpha_{i1} - \nu_{ir}, \alpha_{i1}(0) = \nu_{ir}(0), \tag{12}$$

where $\gamma_{i1} > 0$.

Step 2. The second surface tracking error z_{i2} is defined as follows:

$$z_{i2} = \nu_i - \nu_{ir}. \tag{13}$$

Its time derivative with (2) can be described by

$$M_i\dot{z}_{i2} = \tau_i - f_i(\xi_i, t) - M_i\dot{\nu}_{ir}, \tag{14}$$

where $f_i(\xi_i, t) = C_i(\nu_i)\nu_i + D_i(\nu_i)\nu_i - R^{\mathrm{T}}(\psi_i)\tau_{iw}(t)$, and $\xi_i = [1, \eta_i^{\mathrm{T}}, \nu_i^{\mathrm{T}}]^{\mathrm{T}}$.

When the function $f_i(\xi_i, t)$ is perfectly known, a desired kinetic control law can be chosen as follows:

$$\tau_i = -k_{i2}z_{i2} + f_i(\xi_i, t) + M_i\dot{\nu}_{ir}, \tag{15}$$

where $k_{i2} = \mathrm{diag}\{k_{i21}, k_{i22}, k_{i23}\}$ with $k_{i21} \in \mathbb{R}$, $k_{i22} \in \mathbb{R}$, $k_{i23} \in \mathbb{R}$ being positive constants.

In practice, an accurate knowledge of $f_i(\xi_i, t)$ may not be available; hence, additional schemes should be developed. Before constructing the kinetic control law, the following assumption is required.

Assumption 2. The function $f_i(\xi_i, t)$ can be represented by an NN as

$$f_i(\xi_i, t) = W_i^{\mathrm{T}}(t)\varphi_i(\xi_i) + \epsilon_i(\xi_i), \quad \forall \xi_i \in \mathcal{D}, \tag{16}$$

where $W_i(t)$ is an unknown time-varying matrix satisfying $\|W_i(t)\|_F \leqslant W_i^*$ and $\|\dot{W}_i\|_F \leqslant W_{id}^*$ with $W_i^* \in \mathbb{R}, W_{id}^* \in \mathbb{R}$ being positive constants; $\varphi_i(\xi_i) : \mathcal{D} \to \mathbb{R}^s$ is a known vector function of the form $\varphi_i(\xi_i) = [b_i, \varphi_{i1}(\xi_i), \varphi_{i2}(\xi_i), \ldots, \varphi_{is}(\xi_i)]^{\mathrm{T}}$ satisfying $\|\varphi_i\| \leqslant \varphi_i^*$ with φ_i^* a positive constant, and $\mathcal{D}$ is a compact set; $\epsilon_i(\xi_i)$ is the reconstruction error satisfying $\|\epsilon_i(\xi_i)\| \leqslant \epsilon_i^*$ with ϵ_i^* a positive constant.

Remark 4. A bias term $b_i > 0$ in $\varphi_i(\xi_i)$ is introduced, and it captures the effect of external disturbances imposed on vehicle dynamics. If the NN is replaced by fuzzy logic systems [57, 58], similar results can be derived without any difficulty.

Then, a practical kinetic controller is proposed as follows:

$$\tau_i = -k_{i2}z_{i2} + M_i\dot{\nu}_{ir} + \hat{W}_i^{\mathrm{T}}\varphi_i(\xi_i), \tag{17}$$

where $\hat{W}_i$ is an estimate of W_i.

Following the classical NDSC approach [44, 45], the adaptive law for W_i is directly given by

$$\dot{\hat{W}}_i = \mathit{\Gamma}_i[\varphi_i(\xi_i)z_{i2}^{\mathrm{T}} - k_W\hat{W}_i], \tag{18}$$

where $k_W \in \mathbb{R}$ and $\mathit{\Gamma}_i \in \mathbb{R}$ are positive constants.

The stability properties of close-loop signals using NDSC approach can be established as in [44, 45]. However, the above adaptive control scheme may suffer from the poor learning transient, which can be speculated as follows: First, in order to achieve the desired performance in the presence of large system uncertainties, high-gain learning rates $\mathit{\Gamma}_i$ are necessary for the neural updating law (18). However, adaptive laws using high-gain learning rates may cause signals of high-frequency oscillations, which may exceed the bandwidth of the actuators, and even result in instability for practical applications [52–54]. Second, the tracking error z_{i2} can be nonzero during transient state, which may deteriorate the learning phase and result in control signals of large-magnitude that are unacceptable for actuators. To overcome the above long standing obstacles in NDSC approach, a new updating scheme is developed in this paper, which is capable of achieving smooth and fast learning without generating high-frequency oscillations and yields improved transient performance.

Let $\hat{\nu}_i$ be an estimate of ν_i, and a state predictor is proposed as follows:

$$M_i\dot{\hat{\nu}}_i = -\hat{W}_i^{\mathrm{T}}\varphi_i(\xi_i) + \tau_i - (h_{i1} + k_{i2})\tilde{\nu}_i, \tag{19}$$

where $\tilde{\nu}_i = \hat{\nu}_i - \nu_i$ and $h_{i1} = \mathrm{diag}\{h_{i11}, h_{i12}, h_{i13}\}$ with $h_{i11} \in \mathbb{R}, h_{i12} \in \mathbb{R}, h_{i13} \in \mathbb{R}$ being positive constants.

The update law for $\hat{W}_i$ is designed as

$$\dot{\hat{W}}_i = \mathit{\Gamma}_i[\varphi_i(\xi_i)\tilde{\nu}_i^{\mathrm{T}} - k_W\hat{W}_i]. \tag{20}$$

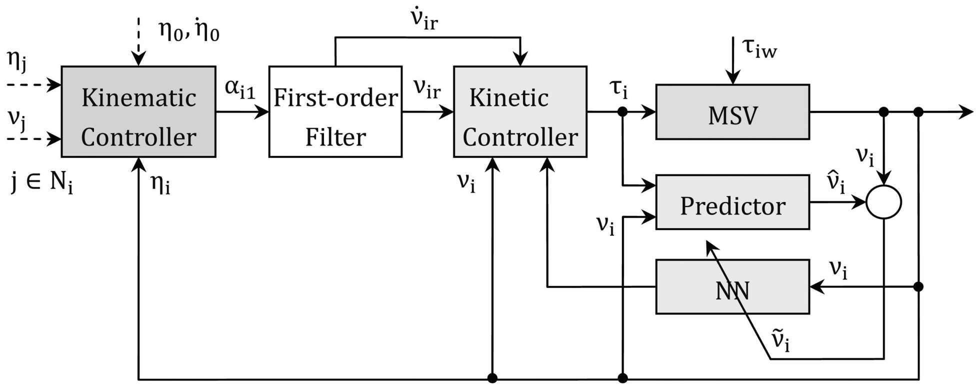

Figure 2 Distributed formation control architecture.

The resulting closed-loop network can be written by

$$\begin{cases} \dot{z}_{i1} &= -r_i S z_{i1} - k_{i1} z_{i1} + a_{id}(-\tilde{\nu}_i + \hat{z}_{i2} + q_{i1}), \\ M_i \dot{\tilde{\nu}}_i &= -(h_{i1} + k_{i2})\tilde{\nu}_i - \tilde{W}_i^{\mathrm{T}} \varphi_i(\xi_i) + \epsilon_i, \\ M_i \dot{\hat{z}}_{i2} &= -k_{i2}\hat{z}_{i2} - h_{i1}\tilde{\nu}_i, \end{cases} \tag{21}$$

where $q_{i1} = \nu_{ir} - \alpha_{i1}$, $\hat{z}_{i2} = \hat{\nu}_i - \nu_{ir}$, and $\tilde{W}_i = \hat{W}_i - W_i$.

Taking the time derivative of q_{i1} and using (12), we have $\dot{q}_{i1} = -q_{i1}/\gamma_{i1} - \dot{\alpha}_{i1}$, whose solution is $q_{i1}(t) = \mathrm{e}^{-\frac{t}{\gamma_{i1}}} q_{i1}(0) - \int_0^t \mathrm{e}^{-\frac{t-\tau}{\gamma_{i1}}} \dot{\alpha}_{i1}(\tau)\mathrm{d}\tau$.

Then, we can compute an upper bound for q_{i1} as

$$\|q_{i1}(t)\| \leqslant \mathrm{e}^{-\frac{t}{\gamma_{i1}}} \|q_{i1}(0)\| + \gamma_{i1}\alpha_{i1d}^*, \tag{22}$$

where α_{i1d}^* is the upper bound for $\dot{\alpha}_{i1}$. Note that the bound for $\dot{\alpha}_{i1}$ exists as long as the inputs are bounded. Since the energy to drive the vehicles is limited, the boundedness of $\dot{\alpha}_{i1}$ is naturally satisfied for practical marine applications.

Remark 5. When setting $q_{i1}(0) = 0$, there exists a positive constant q_{i1}^* such that $\|q_{i1}\| \leqslant q_{i1}^*$ with $q_{i1}^* = \gamma_{i1}\alpha_{i1d}^*$. By decreasing γ_{i1}, the bound for q_{i1} can be reduced accordingly.

To illustrate, a visualization of the distributed formation control architecture for the ith MSV is given in Figure 2. For the ith MSV, it receives the position and velocity information from its neighbors and makes decision based on neighborhood information. Local NNs based on its own states are used to identify the vehicle dynamics. A key feature of the suggested control scheme is that the prediction errors are used to update the NN adaptive laws at the kinetic level, which enables smooth and fast learning, not only in steady state, but also in transient state.

3.2 Stability analysis

Theorem 1. Consider the closed-loop networked system consisting of the vehicle dynamics (1) (2), the control law (17), the adaptive law (20), the first-order filter (12), together with the predictor (19) under Assumptions 1 and 2. Then, all signals in the closed-loop system are uniformly ultimately bounded (UUB), and inequalities (4) and (5) hold for some constants δ_1 and δ_2, provided that the control parameters are selected to satisfy

$$\begin{cases} \kappa_{i11} = \lambda_{\min}(k_{i1}) - \dfrac{3a_{id}}{2} > 0, \\ \kappa_{i12} = \lambda_{\min}(k_{i2}) - \dfrac{a_{id}+1}{2} - \dfrac{\lambda_{\max}(h_{i1})}{2} > 0, \\ \kappa_{i13} = \lambda_{\min}(h_{i1} + k_{i2}) - \dfrac{\lambda_{\max}(h_{i1})+1}{2} > 0, \\ \kappa_{i14} = \dfrac{k_W}{2} - \dfrac{1}{2\Gamma_i} > 0. \end{cases} \tag{23}$$

Proof. Consider the Lyapunov function candidate

$$V_1(z_{i1}, \hat{z}_{i2}, \tilde{\nu}_i, \tilde{W}_i) = \frac{1}{2}\sum_{i=1}^{N}\Big\{z_{i1}^{\rm T}z_{i1} + \hat{z}_{i2}^{\rm T}M_i\hat{z}_{i2} + \tilde{\nu}_i^{\rm T}M_i\tilde{\nu}_i + \varGamma_i^{-1}{\rm tr}(\tilde{W}_i^{\rm T}\tilde{W}_i)\Big\}. \tag{24}$$

Its time derivative along (21) can be expressed as

$$\begin{aligned}\dot{V}_1 \leqslant \sum_{i=1}^{N}\Big\{ &- z_{i1}^{\rm T}k_{i1}z_{i1} + a_{id}z_{i1}^{\rm T}(-\tilde{\nu}_i + \hat{z}_{i2} + q_{i1}) - \hat{z}_{i2}^{\rm T}k_{i2}\hat{z}_{i2} - \hat{z}_{i2}^{\rm T}h_{i1}\tilde{\nu}_i \\ &- \tilde{\nu}_i^{\rm T}(h_{i1} + k_{i2})\tilde{\nu}_i - k_W tr(\tilde{W}_i^{\rm T}\hat{W}_i) + \tilde{\nu}_i^{\rm T}\epsilon_i - \varGamma_i^{-1}tr(\tilde{W}_i^{\rm T}\dot{W}_i)\Big\}. \end{aligned} \tag{25}$$

Using the following inequalities $|\tilde{\nu}_i^{\rm T}\epsilon_i| \leqslant \frac{1}{2}\|\tilde{\nu}_i\|^2 + \frac{1}{2}\epsilon_i^{*2}$, $|z_{i1}^{\rm T}q_{i1}| \leqslant \frac{1}{2}\|z_{i1}\|^2 + \frac{1}{2}q_{i1}^{*2}$, $|z_{i1}^{\rm T}\hat{z}_{i2}| \leqslant \frac{1}{2}\|z_{i1}\|^2 + \frac{1}{2}\|\hat{z}_{i2}\|^2$, $|z_{i1}^{\rm T}\tilde{\nu}_i| \leqslant \frac{1}{2}\|z_{i1}\|^2 + \frac{1}{2}\|\tilde{\nu}_i\|^2$, $\varGamma_i^{-1}{\rm tr}(\tilde{W}_i^{\rm T}\dot{W}_i) \leqslant \frac{1}{2\varGamma_i}\|\tilde{W}_i\|_F^2 + \frac{1}{2\varGamma_i}W_{id}^{*2}$, $-k_W{\rm tr}(\tilde{W}_i^{\rm T}\hat{W}_i) \leqslant -\frac{k_W}{2}\|\tilde{W}_i\|_F^2 + \frac{k_W}{2}W_i^{*2}$, $\hat{z}_{i2}^{\rm T}h_{i1}\tilde{\nu}_i \leqslant \frac{\lambda_{\max}(h_{i1})}{2}\|\hat{z}_{i2}\|^2 + \frac{\lambda_{\max}(h_{i1})}{2}\|\tilde{\nu}_i\|^2$, it can be followed from (25) that

$$\begin{aligned}\dot{V}_1 \leqslant \sum_{i=1}^{N}\Big\{ &- \Big(\lambda_{\min}(k_{i1}) - \frac{3a_{id}}{2}\Big)z_{i1}^{\rm T}z_{i1} - \Big(\lambda_{\min}(k_{i2}) - \frac{a_{id}+1}{2} - \frac{\lambda_{\max}(h_{i1})}{2}\Big)\hat{z}_{i2}^{\rm T}\hat{z}_{i2} \\ &- \Big(\frac{k_W}{2} - \frac{1}{2\varGamma_i}\Big)\|\tilde{W}_i\|_F^2 - \Big(\lambda_{\min}(h_{i1} + k_{i2}) - \frac{\lambda_{\max}(h_{i1}) + 1}{2}\Big)\tilde{\nu}_i^{\rm T}\tilde{\nu}_i\Big\} + \varepsilon_1, \end{aligned} \tag{26}$$

where $\varepsilon_1 = \sum_{i=1}^{N}\{\frac{1}{2}\epsilon_i^{*2} + \frac{1}{2}q_{i1}^{*2} + \frac{k_W}{2}W_i^{*2} + \frac{1}{2\varGamma_i}W_{id}^{*2}\}$.

Using (23) and letting $\kappa_1 = \min_{i=1,\ldots,N}\{2\kappa_{i11}, 2\kappa_{i12}/\lambda_{\max}(M_i), 2\kappa_{i13}/\lambda_{\max}(M_i), 2\kappa_{i14}\varGamma_i\}$, the inequality (26) becomes

$$\dot{V}_1 \leqslant -\kappa_1 V_1 + \varepsilon_1. \tag{27}$$

Therefore, all signals in the closed-loop network (e.g., z_{i1}, $\hat{z}_{i2}$, $\tilde{W}_i$, $\tilde{\nu}_i$) are UUB [59]. Solving the inequality (27) gives

$$V_1 \leqslant \frac{\varepsilon_1}{\kappa_1}\Big(1 - {\rm e}^{-\kappa_1 t}\Big) + V_1(0){\rm e}^{-\kappa_1 t}. \tag{28}$$

Note that $\|z_1\|^2/2 \leqslant V_1$, and then

$$\|z_1\|^2 \leqslant \frac{2\varepsilon_1}{\kappa_1}\Big(1 - {\rm e}^{-\kappa_1 t}\Big) + 2V_1(0){\rm e}^{-\kappa_1 t},$$

from which we derive that the tracking error $\|z_1\| \leqslant \sqrt{2\varepsilon_1/\kappa_1}$ as $t \to \infty$. By Lemma 1 and Assumption 1, one has $\|s_i\| \leqslant \frac{1}{\underline{\sigma}(\mathcal{H})}\sqrt{2\varepsilon_1/\kappa_1}$ as $t \to \infty$. In addition, note that $\|\eta_i - \eta_j - \mathcal{P}_{ij}\| \leqslant \|s_i\| + \|s_j\|$, then Eq. (4) is satisfied with $\delta_1 = \frac{2}{\underline{\sigma}(\mathcal{H})}\sqrt{2\varepsilon_1/\kappa_1}$.

Since $\|\sum_{i=1}^{N}\frac{\eta_i}{N} - \eta_0\| \leqslant \frac{\sum_{i=1}^{N}\|z_{i1}\|}{N}$, it implies (5) with $\delta_2 = \frac{1}{\underline{\sigma}(\mathcal{H})}\sqrt{2\varepsilon_1/\kappa_1}$.

By appropriately increasing the parameter κ_1, the bounds δ_1 and δ_2 can be reduced. The proof is complete.

Remark 6. In a related work [10], leader-follower formation controllers were developed for MSVs based on the NDSC approach. Compared to [10], the differences are two-fold. First, the work in [10] considers the formation control of MSVs being lack of sharing information; while in this paper, distributed formation controllers based on information of neighbors are constructed. Second, the proposed PNDSC design approach results in new distributed formation controllers.

3.3 Transient analysis

In the following section, we quantify the transient performance of the proposed method by deriving truncated L_2 norm of $\dot{W}_i$. This metric relates to the frequency characteristics of a signal [60]. Generally, a larger L_2 norm of $\dot{W}_i$ in a specified time duration implies more oscillations contained in the signal of W_i. In this subsection, we show that the L_2 norm of $\dot{W}_i$ of the proposed PNDSC architecture is smaller than that of NDSC approach by selecting the parameter h_{i1}, and thus yields the improved transient performance.

3.3.1 *Transient analysis using PNDSC approach*

Recalling (21), the prediction error dynamics of $\tilde{\nu}_i$ can be written as

$$M_i\dot{\tilde{\nu}}_i = -(h_{i1}+k_{i2})\tilde{\nu}_i - \tilde{W}_i^{\mathrm{T}}\varphi_i(\xi_i) + \epsilon_i. \tag{29}$$

Note that the control signal τ_i serves as an input to both systems, i.e., the plant (2) and the predictor (19); however, the stability of the prediction error dynamics does not depend on the control input τ_i. This means that the estimation loop is decoupled from the control loop since the updating law (20) only depends on the prediction error $\tilde{\nu}_i$.

Here, we first establish the transient property for $\tilde{\nu}_i$ in terms of its truncated L_2 norm; and then, we derive the transient property for $\dot{\hat{W}}_i$ by making use of (20).

Theorem 2. Consider the prediction error dynamics (29) together with the adaptive law (20); then, the truncated L_2 norms of $\tilde{\nu}_i$ and $\dot{\hat{W}}_i$ satisfy

$$\|\tilde{\nu}_i\|_{L_2,t^*} \leqslant \frac{1}{\sqrt{2\lambda_{\min}(h_{i1}+k_{i2})-1}}\left(\sqrt{\lambda_{\max}(M_i)}\|\tilde{\nu}_i(0)\| + \frac{\|\tilde{W}_i(0)\|_F}{\sqrt{\Gamma_i}} + \sqrt{2\varepsilon_1^* t^*}\right), \tag{30}$$

and

$$\begin{aligned}\|\dot{\hat{W}}_i\|_{L_2,t^*} \leqslant{}& \frac{\sqrt{2}\Gamma_i\varphi_i^*}{\sqrt{2\lambda_{\min}(h_{i1}+k_{i2})-1}}\left(\sqrt{\lambda_{\max}(M_i)}\|\tilde{\nu}_i(0)\| + \frac{\|\tilde{W}_i(0)\|_F}{\sqrt{\Gamma_i}} + \sqrt{2\varepsilon_1^* t^*}\right)\\ &+ \sqrt{2}\Gamma_i k_W\left(\sqrt{\frac{2\Gamma_i\varepsilon_1^*}{\kappa_{iT}}} + \sqrt{\lambda_{\max}(M_i)}\|\tilde{\nu}_i(0)\|\sqrt{\Gamma_i} + \|\tilde{W}_i(0)\|_F + W_i^*\right)\sqrt{t^*}.\end{aligned} \tag{31}$$

Proof. Consider the following Lyapunov function candidate

$$V(t) = \frac{1}{2}\tilde{\nu}_i^{\mathrm{T}}M_i\tilde{\nu}_i + \frac{1}{2\Gamma_i}\mathrm{tr}(\tilde{W}_i^{\mathrm{T}}\tilde{W}_i). \tag{32}$$

The time derivative of $V(t)$ along (20) and (29) is given by

$$\dot{V}(t) = -\tilde{\nu}_i^{\mathrm{T}}(h_{i1}+k_{i2})\tilde{\nu}_i - k_W\mathrm{tr}(\tilde{W}_i^{\mathrm{T}}\hat{W}_i) + \tilde{\nu}_i^{\mathrm{T}}\epsilon_i - \Gamma_i^{-1}\mathrm{tr}(\tilde{W}_i^{\mathrm{T}}\dot{W}_i), \tag{33}$$

which can be further formed into

$$\dot{V}(t) \leqslant -\Big(\lambda_{\min}(h_{i1}+k_{i2}) - \frac{1}{2}\Big)\tilde{\nu}_i^{\mathrm{T}}\tilde{\nu}_i - \Big(\frac{k_W}{2} - \frac{1}{2\Gamma_i}\Big)\|\tilde{W}_i\|_F^2 + \varepsilon_1^*, \tag{34}$$

where $\varepsilon_1^* = \frac{1}{2}\epsilon_i^{*2} + \frac{k_W}{2}W_i^{*2} + \frac{1}{2\Gamma_i}W_{id}^{*2}$.

Letting $\kappa_{iT} = \min\{2\lambda_{\min}(h_{i1}+k_{i2})-1, \Gamma_i k_W - 1\} > 0$, the inequality (34) can be written as $\dot{V}(t) \leqslant -\kappa_{iT}V(t) + \varepsilon_1^*$, whose solution is

$$V(t) \leqslant \frac{\varepsilon_1^*}{\kappa_{iT}}\Big(1 - \mathrm{e}^{-\kappa_{iT}t}\Big) + V(0)\mathrm{e}^{-\kappa_{iT}t}. \tag{35}$$

Similarly, we can derive that $\|\tilde{\nu}_i\|$ and $\|\tilde{W}_i\|$ are bounded by

$$\|\tilde{\nu}_i\| \leqslant \frac{1}{\sqrt{\lambda_{\min}(M_i)}}\left(\sqrt{\frac{2\varepsilon_1^*}{\kappa_{iT}}} + \sqrt{\lambda_{\max}(M_i)}\|\tilde{\nu}_i(0)\| + \frac{\|\tilde{W}_i(0)\|_F}{\sqrt{\Gamma_i}}\right) \tag{36}$$

and

$$\|\tilde{W}_i\|_F \leqslant \sqrt{\Gamma_i}\left(\sqrt{\frac{2\varepsilon_1^*}{\kappa_{iT}}} + \sqrt{\lambda_{\max}(M_i)}\|\tilde{\nu}_i(0)\| + \frac{\|\tilde{W}_i(0)\|_F}{\sqrt{\Gamma_i}}\right), \tag{37}$$

where the inequality $\sqrt{a+b} \leqslant \sqrt{a} + \sqrt{b}$ with $a \geqslant 0$ and $b \geqslant 0$ has been used.

Recalling the inequality (34), we obtain

$$\left(\lambda_{\min}(h_{i1}+k_{i2})-\frac{1}{2}\right)\|\tilde{\nu}_i\|^2 \leqslant -\dot{V}(t)+\varepsilon_1^*, \tag{38}$$

by integration of which over $t\in[0,t^*]$ gives

$$\|\tilde{\nu}_i\|_{L_2,t^*}^2 \leqslant \frac{V(0)}{\lambda_{\min}(h_{i1}+k_{i2})-1/2}+\frac{\varepsilon_1^* t^*}{\lambda_{\min}(h_{i1}+k_{i2})-1/2}. \tag{39}$$

Noting that

$$\sqrt{V(0)} \leqslant \frac{\sqrt{\lambda_{\max}(M_i)}}{\sqrt{2}}\|\tilde{\nu}_i(0)\|+\frac{\|\tilde{W}_i(0)\|_F}{\sqrt{2\Gamma_i}}, \tag{40}$$

one has (30).

Next, we explicitly derive the upper bound for $\|\dot{\hat{W}}_i\|$. To this end, recalling the expression of $\dot{\hat{W}}_i$ in (20), we have

$$\|\dot{\hat{W}}_i\|_F \leqslant \Gamma_i\|\varphi_i(\xi_i)\|\|\tilde{\nu}_i\|+\Gamma_i k_W\|\hat{W}_i\|_F. \tag{41}$$

Using the bounds for $\varphi_i(\xi_i)$ and W_i and noting (37), we have

$$\|\dot{\hat{W}}_i\|_F \leqslant \Gamma_i\varphi_i^*\|\tilde{\nu}_i\|+\Gamma_i k_W(\tilde{W}_i^*+W_i^*), \tag{42}$$

which results in

$$\|\dot{\hat{W}}_i\|_{L_2,t^*}^2 \leqslant 2\Gamma_i^2\varphi_i^{*2}\|\tilde{\nu}_i\|_{L_2,t^*}^2+2\Gamma_i^2 k_W^2(\tilde{W}_i^*+W_i^*)^2 t^*, \tag{43}$$

where $\tilde{W}_i^*=\sqrt{\Gamma_i}(\sqrt{2\varepsilon_1^*/\kappa_{iT}}+\sqrt{\lambda_{\max}(M_i)}\|\tilde{\nu}_i(0)\|+\|\tilde{W}_i(0)\|_F/\sqrt{\Gamma_i})$. Here, we can obtain

$$\|\dot{\hat{W}}_i\|_{L_2,t^*} \leqslant \sqrt{2}\Gamma_i\varphi_i^*\|\tilde{\nu}_i\|_{L_2,t^*}+\sqrt{2}\Gamma_i k_W(\tilde{W}_i^*+W_i^*)\sqrt{t^*}. \tag{44}$$

From (30) and (37), we finally have (31).

Remark 7. From (30) and (31), it is clear that by increasing $\lambda_{\min}(h_{i1})$, one can decrease the L_2 norms of $\tilde{\nu}_i$ and $\dot{\hat{W}}_i$; i.e., reduce the oscillations in neural adaptive control signals.

Remark 8. The state of the predictor (19) can be easily initialized such that $\hat{\nu}_i(0)=\nu_i(0)$; then, the truncated L_2 norms of $\tilde{\nu}_i$ and $\dot{\hat{W}}_i$ are

$$\|\tilde{\nu}_i\|_{L_2,t^*} \leqslant \frac{1}{\sqrt{2\lambda_{\min}(h_{i1}+k_{i2})-1}}\left(\frac{\|\tilde{W}_i(0)\|_F}{\sqrt{\Gamma_i}}+\sqrt{2\varepsilon_1^* t^*}\right), \tag{45}$$

and

$$\begin{aligned}\|\dot{\hat{W}}_i\|_{L_2,t^*} \leqslant{}& \frac{\sqrt{2}\Gamma_i\varphi_i^*}{\sqrt{2\lambda_{\min}(h_{i1}+k_{i2})-1}}\left(\frac{\|\tilde{W}_i(0)\|_F}{\sqrt{\Gamma_i}}+\sqrt{2\varepsilon_1^* t^*}\right)\\ &+\sqrt{2}\Gamma_i k_W\left(\sqrt{\frac{2\Gamma_i\varepsilon_1^*}{\kappa_{iT}}}+\|\tilde{W}_i(0)\|_F+W_i^*\right)\sqrt{t^*}.\end{aligned} \tag{46}$$

3.3.2 *Transient analysis using NDSC approach*

In order to explicitly demonstrate the transient performance improvement of the proposed method, we derive the truncated L_2 norm of $\dot{\hat{W}}_i$ using the NDSC approach.

By substituting the control law (17) into (14), we derive

$$M_i\dot{z}_{i2}=-k_{i2}z_{i2}-\tilde{W}_i^{\mathrm{T}}\varphi_i(\xi_i)+\epsilon_i. \tag{47}$$

In light of the updating law (18), one can find that the estimation loop is coupled with the control loop, since the convergence of tracking error z_{i2} influences the learning behavior of NN.

The following corollary is straightforward by taking $h_{i1} = 0$ and replacing $\tilde{\nu}_i$ with z_{i2} in proving the Theorem 2.

Corollary 1. Consider the error dynamics of z_{i2} together with the adaptive law (20); then, the truncated L_2 norms of z_{i2} and $\dot{\hat{W}}_i$ satisfy

$$\|z_{i2}\|_{L_2,t^*} \leqslant \frac{1}{\sqrt{2\lambda_{\min}(k_{i2})-1}}\left(\sqrt{\lambda_{\max}(M_i)}\|z_{i2}(0)\| + \frac{\|\tilde{W}_i(0)\|_F}{\sqrt{\Gamma_i}} + \sqrt{2\varepsilon_1^* t^*}\right) \tag{48}$$

and

$$\begin{aligned}\|\dot{\hat{W}}_i\|_{L_2,t^*} \leqslant{}& \frac{\sqrt{2}\Gamma_i\varphi_i^*}{\sqrt{2\lambda_{\min}(k_{i2})-1}}\left(\sqrt{\lambda_{\max}(M_i)}\|z_{i2}(0)\| + \frac{\|\tilde{W}_i(0)\|_F}{\sqrt{\Gamma_i}} + \sqrt{2\varepsilon_1^* t^*}\right)\\ &+ \sqrt{2}\Gamma_i k_W\left(\sqrt{\frac{2\Gamma_i\varepsilon_1^*}{\kappa_{iT}}} + \sqrt{\lambda_{\max}(M_i)}\|z_{i2}(0)\|\sqrt{\Gamma_i} + \|\tilde{W}_i(0)\|_F + W_i^*\right)\sqrt{t^*}.\end{aligned} \tag{49}$$

Proof. Omitted here.

Remark 9. From (48) and (49), we find that one possible way to decrease L_2 norm of $\dot{\hat{W}}_i$ is by decreasing Γ_i. This results in the classic trade-off performance in neural adaptive control. By choosing a small adaptive gain Γ_i, the oscillations in the neural weight $\hat{W}_i$ can be reduced; however, this will results in poor tracking performance of z_{i2}. Besides, note that z_{i2} cannot be initialized to be zero to deduce its impact on $\|\dot{\hat{W}}_i\|_{L_2,t^*}$. In short, compared with the NDSC approach, the proposed PNDSC architecture provides two avenues (extra freedom) to improve the transient performance of NN-based DSC design in terms of decreasing the L_2 norms of key adaptive signals. One is done by increasing the parameters $\lambda_{\min}(h_{i1})$; and the other is by initializing $\hat{\nu}_i(0) = \nu_i(0)$.

4 DFT without using neighbors' velocity information

In the previous section, both the velocity and position information of neighbors are required for controller design. However, from a practical perspective, it is desirable to only use the position information of neighboring vehicles because the velocity information may not be available in some circumstances. On the other hand, using position information alone may be helpful in decreasing the network burden. In addition, note that as observed in nature, each individual is able to sense the positions of its neighbors, and the velocities must be estimated or evaluated by their local controllers. Therefore, the control objective of this section is to achieve the DFT without using velocity information of neighbors. In this section, we continue to use the notations defined in the previous section. If they need to be changed, we redefine them explicitly.

4.1 Controller design

Rewrite the dynamics of z_{i1} as

$$\dot{z}_{i1} = -r_i S z_{i1} + a_{id}[\nu_i - \omega_i(t)], \tag{50}$$

where $\omega_i(t)$ is expressed by

$$\omega_i(t) = \frac{\sum_{j=1}^N a_{ij} R_i^{\mathrm{T}} R_j \nu_j(t) + a_{i0} R_i^{\mathrm{T}} \dot{\eta}_0(t)}{a_{id}}, \tag{51}$$

which is treated as a composite disturbance imposed on the system. Since the vehicles are mechanical systems, subject to Newton's second law, their velocities and accelerations are reasonably bounded. Therefore, there exist positive constants $\omega_i^* \in \mathbb{R}$ and $\omega_{id}^* \in \mathbb{R}$ such that $\|\omega_i(t)\| < \omega_i^*$ and $\|\dot{\omega}_i(t)\| < \omega_{id}^*$.

Consider a state predictor as follows:

$$\dot{\hat{z}}_{i1} = -r_i S\hat{z}_{i1} + a_{id}[\nu_i - \hat{\omega}_i(t)] - (h_{i2} + k_{i1})\tilde{z}_{i1}, \tag{52}$$

where $\tilde{z}_{i1} = \hat{z}_{i1} - z_{i1}$; $\hat{\omega}_i(t)$ is an estimate of $\omega_i(t)$; $h_{i2} = \mathrm{diag}\{h_{i21}, h_{i22}, h_{i23}\}$ with $h_{i21} \in \mathbb{R}, h_{i22} \in \mathbb{R}, h_{i23} \in \mathbb{R}$ being positive constants.

The update law for $\hat{\omega}_i(t)$ is given by

$$\dot{\hat{\omega}}_i(t) = \mathit{\Gamma}_{i\omega}[a_{id}\tilde{z}_{i1} - k_\omega \hat{\omega}_i(t)], \tag{53}$$

where $\mathit{\Gamma}_{i\omega} \in \mathbb{R}$ and $k_\omega \in \mathbb{R}$ are positive constants.

With the developed predictor, a virtual control law α_{i2} is proposed as follows:

$$\alpha_{i2} = -\frac{k_{i1}}{a_{id}} z_{i1} + \hat{\omega}_i(t). \tag{54}$$

Let α_{i2} pass through a first-order filter bank with a time constant $\gamma_{i2} \in \mathbb{R}$ to obtain the filtered control signal ν_{ir} as follows:

$$\gamma_{i2}\dot{\nu}_{ir} = \alpha_{i2} - \nu_{ir}, \alpha_{i2}(0) = \nu_{ir}(0), \tag{55}$$

where $\gamma_{i2} > 0$.

The resulting closed-loop system can be described by

$$\begin{cases} \dot{\hat{z}}_{i1} & = -r_i S\hat{z}_{i1} - k_{i1}\hat{z}_{i1} - h_{i2}\tilde{z}_{i1} + a_{id}(-\tilde{\nu}_i + \hat{z}_{i2} + q_{i2}), \\ \dot{\tilde{z}}_{i1} & = -r_i S\tilde{z}_{i1} - (h_{i2} + k_{i1})\tilde{z}_{i1} - a_{id}\tilde{\omega}_i(t), \\ M_i\dot{\hat{z}}_{i2} & = -k_{i2}\hat{z}_{i2} - h_{i1}\tilde{\nu}_i, \\ M_i\dot{\tilde{\nu}}_i & = -(h_{i1} + k_{i2})\tilde{\nu}_i - \tilde{W}_i^{\mathrm{T}}\varphi_i(\xi_i) + \epsilon_i, \end{cases} \tag{56}$$

where $q_{i2} = \nu_{ir} - \alpha_{i2}$, and $\|q_{i2}\| \leqslant q_{i2}^*$ with q_{i2}^* being a constant.

4.2 Stability analysis

Theorem 3. Consider the closed-loop networked system consisting of the vehicle dynamics (1) (2), the control law (17) (54), the adaptive law (20) (53), the first-order filter (55), together with the predictor (19) (52) under Assumptions 1 and 2. Then, all signals in the closed-loop system are UUB, and the inequalities (4) and (5) hold for some constants δ_1 and δ_2, provided that the control parameters are selected to satisfy

$$\begin{cases} \kappa_{i21} = \lambda_{\min}(k_{i1}) - \dfrac{3a_{id}}{2} - \dfrac{\lambda_{\max}(h_{i2})}{2} > 0, \\ \kappa_{i22} = \lambda_{\min}(k_{i2}) - \dfrac{a_{id}+1}{2} - \dfrac{\lambda_{\max}(h_{i2})}{2} > 0, \\ \kappa_{i23} = \lambda_{\min}(h_{i1} + k_{i2}) - \dfrac{\lambda_{\max}(h_{i1}) + 1}{2} > 0, \\ \kappa_{i24} = \dfrac{k_W}{2} - \dfrac{1}{2\mathit{\Gamma}_i} > 0, \\ \kappa_{i25} = \lambda_{\min}(h_{i2} + k_{i1}) - \dfrac{\lambda_{\max}(h_{i2}) + 1}{2} > 0, \\ \kappa_{i26} = \dfrac{k_\omega}{2} - \dfrac{1}{2\mathit{\Gamma}_{i\omega}} > 0. \end{cases} \tag{57}$$

Proof. The proof details are similar to the proof of Theorem 1, which are omitted here.

The above procedure illustrates the stability analysis of DFT control without using neighbors' velocity information, and the transient properties of neural adaptive terms can be established as the same as in Subsection 3.3, which are omitted here.

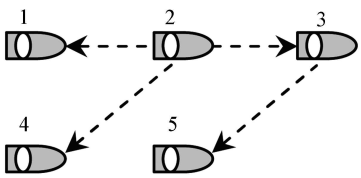

Figure 3 Communication topology.

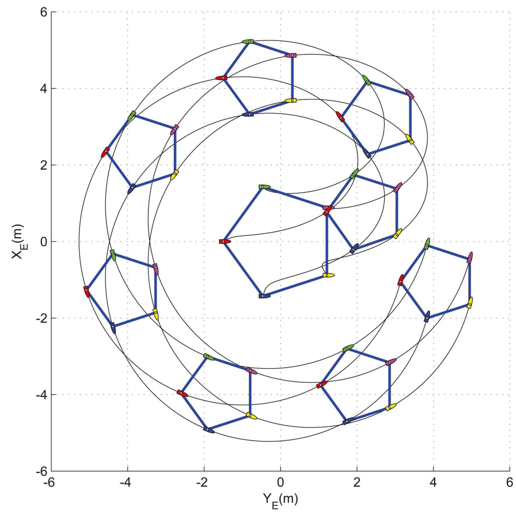

Figure 4 (Color online) Formation trajectories.

Remark 10. In contrast to the previous design where both the position and velocity information of neighboring agents are required, the proposed design in this section only use the relative position information of neighboring agents and its own states. Therefore, the information required to be communicated is reduced. Moreover, this design is also useful for practical applications where only local sensors (e.g., visual sensors) are equipped; i.e., only the relative position information can be available for feedback.

Remark 11. Note that the parameter selection depends on the value of a_{id}, which is connected with the network links. Once the network is determined, the qualified forms of a_{id} will be known; then, k_{i1}, k_{i2}, and k_{i3} can be chosen accordingly. In practical engineering system, k_{i1} and k_{i2} are designed based on the desired output responses. In general, large control gains of k_{i1}, and k_{i2} lead to fast responses. However, they may also result in large control signals in the initial stage. Therefore, a trial and try should be performed to obtain satisfactory performance. As for NN parameters, the adaptive gains Γ_i can be selected as large as possible, subject to the limitations of hardware. h_{i1} and h_{i2} determine the damping of NN learning. Hence, by properly selecting h_{i1}, a smoother approximation can be obtained.

5 An example

Consider a network of marine vehicles whose dynamic is governed by a model ship and its parameters are $m_{11} = 25.8$, $m_{22} = 33.8$, $m_{23} = m_{32} = 1.0948$, $m_{33} = 2.760$, $c_{13} = -c_{31} = -33.8v - 1.0948r$, $c_{23} = -c_{32} = 25.8u$, $d_{11} = 0.72+1.33|u|+5.87u^2$, $d_{22} = 0.8896+36.5|v|+0.805|r|$, $d_{23} = 7.25+0.845|v|+3.45|r|$, $d_{32} = 0.0313 + 3.96|v| + 0.130|r|$, $d_{33} = 1.90 - 0.080|v| + 0.75|r|$. The ocean disturbances are modeled as the first-order Gauss-Markov processes.

A networked system consisting of five MSVs is considered where the communication topology is described by Figure 3 with the vehicle 2 being the leader. The controllers given in Theorem 1 are applied to the vehicle network. The formation shape is set to $\mathcal{P}_1 = [-1, 0, 0]^{\mathrm{T}}$, $\mathcal{P}_2 = [-\cos(2\pi/5), \sin(2\pi/5), 0]^{\mathrm{T}}$, $\mathcal{P}_3 = [-\cos(2\pi/5), -\sin(2\pi/5), 0]^{\mathrm{T}}$, $\mathcal{P}_4 = [\cos(\pi/5), \sin(\pi/5), 0]^{\mathrm{T}}$, $\mathcal{P}_5 = [\cos(\pi/5), -\sin(\pi/5), 0]^{\mathrm{T}}$. The control parameters are chosen as $h_{i1} = \mathrm{diag}\{516, 676, 55.2\}$, $k_{i1} = \mathrm{diag}\{2, 2, 2\}$, $k_{i2} = \mathrm{diag}\{119, 169, 13.8\}$, $\Gamma_i = 10000$, $k_W = 0.001$, and $\gamma_{i1} = 0.02$. To illustrate, the PNDSC scheme is compared with the NDSC approach [44], and the same adaptive parameters are selected for the direct adaptive laws in the NDSC approach.

Figure 4 demonstrates the formation trajectories of the five MSVs, and it can be seen that a star formation is well established despite being disturbed by the model uncertainty and unknown ocean disturbances. In Figure 5, (a) and (b) depict the output response of the NDSC and PNDSC approach, respectively, where $x_i^- = x_i - p_{ix}$, $y_i^- = y_i - p_{iy}$ and $\psi_i^- = \psi_i - p_{i\psi}$. (c) shows the tracking error

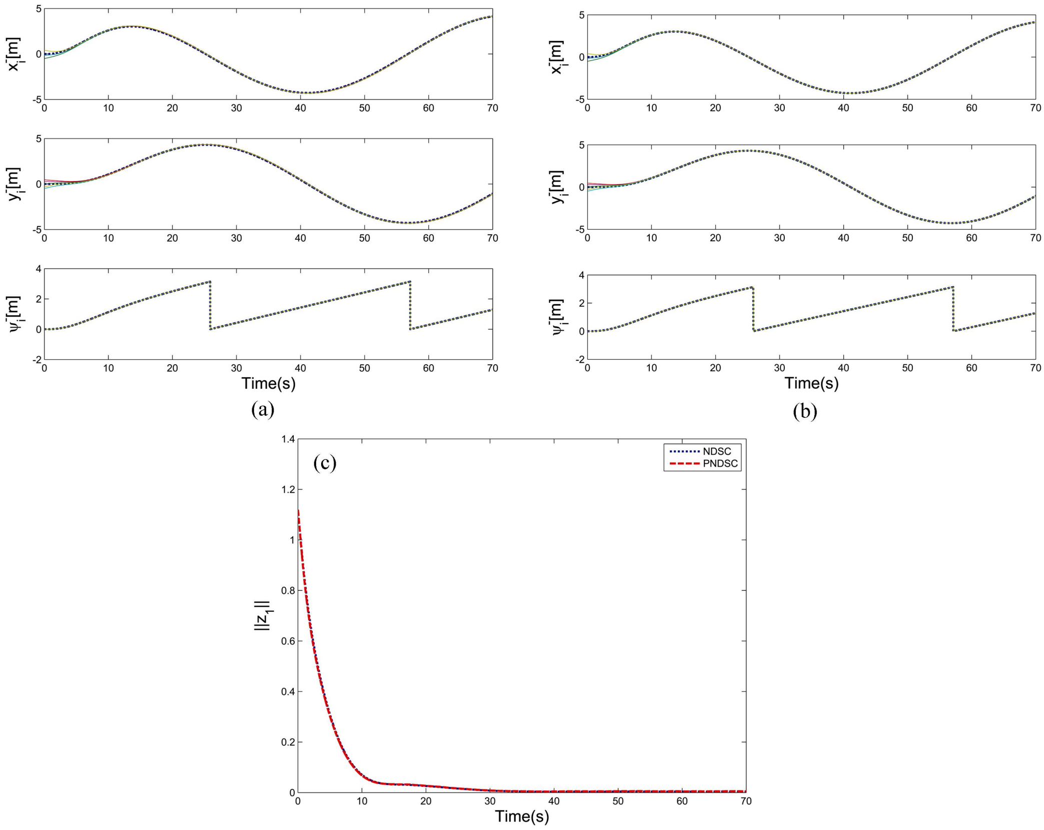

Figure 5 (Color online) Output comparisons of (a) the NDSC and (b) PNDSC approaches. Leader (dot line) and followers (solid line). (c) Tracking error norms of z_1.

norms of z_1, and it reveals that the tracking performance for the PNDSC and NDSC is almost the same, but the transient performance can be quite different. The learning profile of NN using the NDSC and PNDSC approach, respectively, corresponding to the first vehicle, are shown in Figures 6 and 7. Figure 6 demonstrates that the NN is able to capture the unknown vehicle dynamics in the steady state, but experiences poor learning transient. By contrast, Figure 7 shows that a smooth and fast learning process can be reached using the PNDSC approach. The control signals using the NDSC and PNDSC approaches are shown in Figure 8, where it demonstrates that the steady control efforts for the NDSC and PNDSC are the same, however, the PNDSC method has better transient properties than the NDSC approach, with less oscillations in the control signals.

6 Conclusion

In this paper, we considered the DFT problem of multiple MSVs in the presence of model uncertainty and time-varying ocean disturbances. DFT controllers are developed with the aid of a new PNDSC approach. These controllers are designed to ensure that a relative formation among vehicles can be reached in a distributed manner for directed graphs containing a spanning tree. Lyapunov analysis demonstrated that all signals in the closed-loop systems are UUB, and the formation tracking errors converge to a small neighborhood of the origin. An extension to DFT using relative position information is further studied. Comparative studies are given to show the substantial improvements of well known results in the literature. Several possible extensions of the presented work are presented as follows:

- First, we considered the state feedback-based DFT of multiple MSVs in this paper. It will be desirable to extend the result to the output feedback case where only the position information can be available.

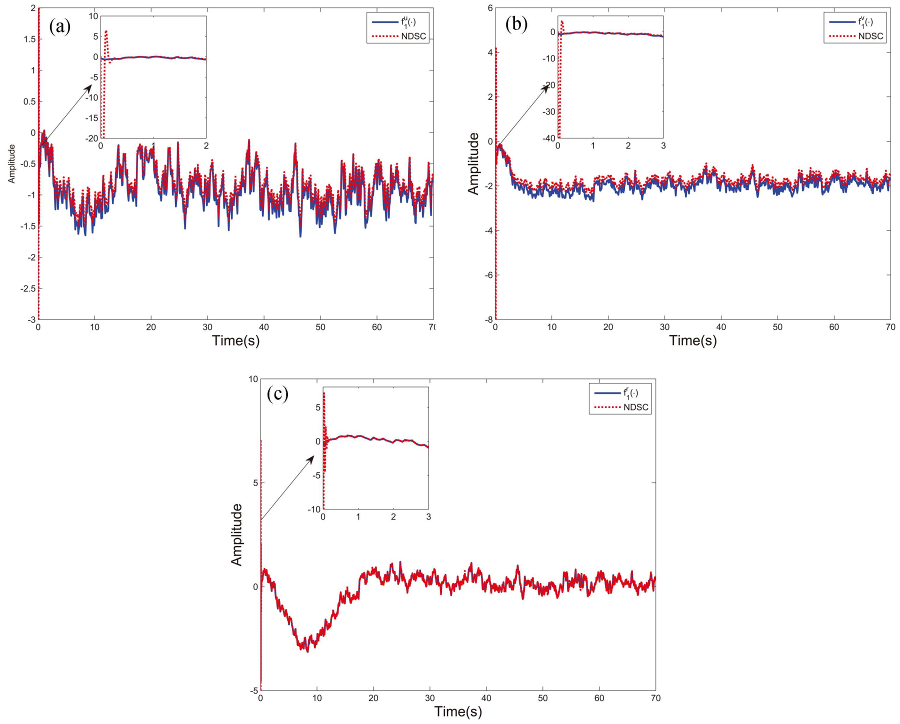

Figure 6 (Color online) Learning profile of NN using the PNDSC. The NN estimation of (a) $f_1^u(\cdot)$ in the surge direction, (b) $f_1^v(\cdot)$ in the sway direction, and (c) $f_1^r(\cdot)$ in the yaw direction.

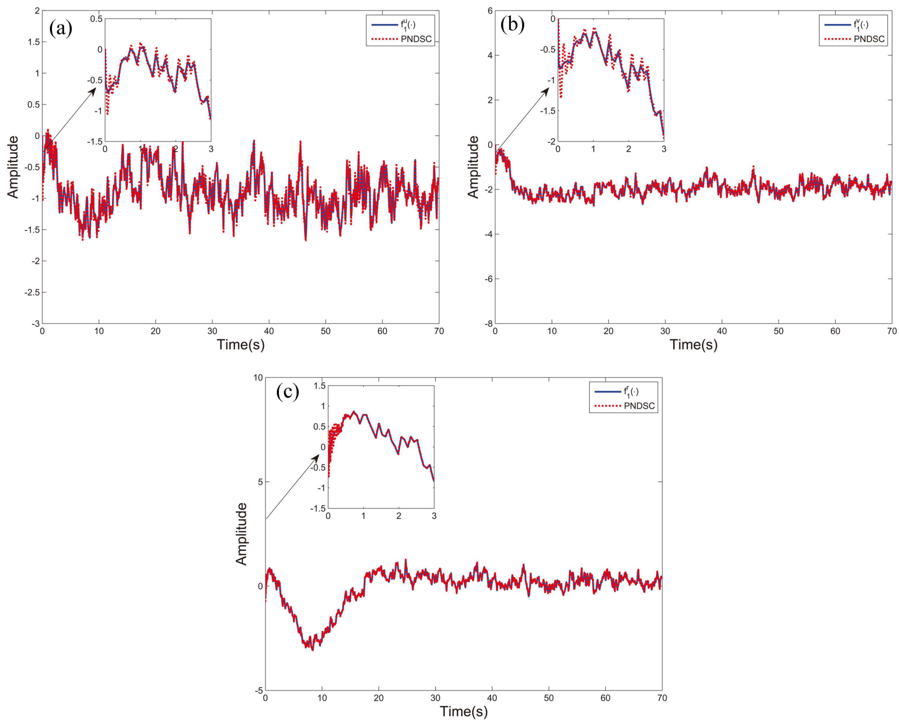

Figure 7 (Color online) Learning profile of NN using the PNDSC. The NN estimation of (a) $f_1^u(\cdot)$ in the surge direction, (b) $f_1^v(\cdot)$ in the sway direction, and (c) $f_1^r(\cdot)$ in the yaw direction.

- Second, in the presented work the reference trajectory η_0 is time dependent. It will be interesting to study DFT of multiple MSVs in the presence of a parameterized trajectory, i.e., distributed path following problem.

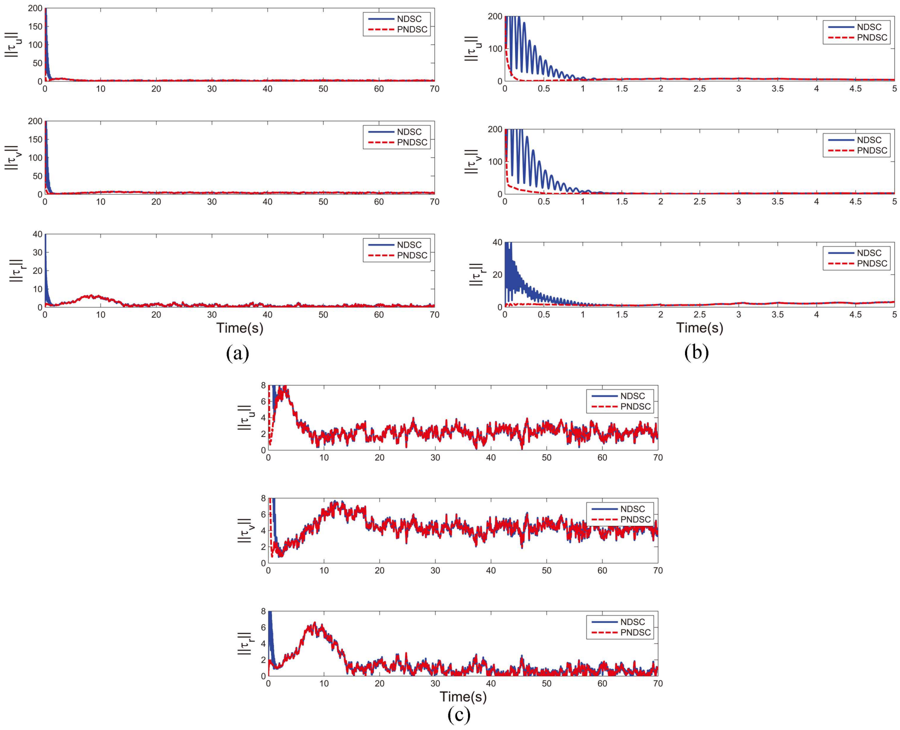

Figure 8 (Color online) Control inputs of the NDSC and PNDSC approaches. (a) Scale limits: Time(0-70), τ_u(0-200), τ_v(0-200), τ_r(0-40); (b) scale limits: Time(0-5), τ_u(0-200), τ_v(0-200), τ_r(0-40); (c) scale limits: Time(0-70), τ_u(0-8), τ_v(0-8), τ_r(0-8).

- Third, the vehicle considered in this paper is fully actuated. An extension to underactuated MSVs will also be addressed in the future work.

Acknowledgements The authors would like to thank the reviewers for their constructive comments, which have improved the quality of this paper. This work was in part supported by National Nature Science Foundation of China (Grants Nos. 51209026, 51179019, 61273137, 51579023, 51579022), China Postdoctoral Science Foundation (Grant No. 2015M570247), Scientific Research Fund of Liaoning Provincial Education Department (Grant No. L2013202), and Fundamental Research Funds for the Central Universities (Grant Nos. 3132015021, 3132014321).

Conflict of interest The authors declare that they have no conflict of interest.

References

1 Jadbabaie A, Lin J, Morse A S. Coordination of groups of mobile autonomous agents using nearest neighbor rules. IEEE Trans Autom Control, 2003, 48: 988–1001
2 Fax J A, Murray R M. Information flow and cooperative control of vehicle formations. IEEE Trans Autom Control, 2004, 49: 1465–1476
3 Skjetne R, Moi S, Fossen T I. Nonlinear formation control of marine craft. In: Proceedings of the 41st IEEE Conference on Decision and Control, Las Vegas, 2002, 2: 1699–1704
4 Ihle I, Arcak F M, Fossen T I. Passivity-based designs for synchronized path following. Automatica, 2007, 43: 1508–1518
5 Almeida J, Silvestre C, Pascoal A M. Cooperative control of multiple surface vessels in the presence of ocean currents and parametric model uncertainty. Int J Robust Nonlin Control, 2010, 20: 1549–1565
6 Breivik M, Hovstein V E, Fossen T I. Ship formation control: a guided leader-follower approach. In: Proceedings of the 17th IFAC World Congress, COEX, 2008, 17: 16008–16014
7 Kyrkjebø E, Pettersen K Y, Wondergem M, et al. Output synchronization control of ship replenishment operations: Theory and experiments. Control Eng Pract, 2007, 15: 741–755
8 Cui R X, Ge S S, How B V E, et al. Leader-follower formation control of underactuated autonomous underwater vehicles. Ocean Eng, 2010, 37: 1491–1502
9 Peng Z H, Wang D, Hu X J. Robust adaptive formation control of underactuated autonomous surface vehicles with uncertain dynamics. IET Control Theory Appl, 2011, 5: 1378–1387

10 Peng Z H, Wang D, Chen Z Y, et al. Adaptive dynamic surface control for formations of autonomous surface vehicles with uncertain dynamics. IEEE Trans Control Syst Tech, 2013, 21: 513–520

11 Arrichiello F, Chiaverini S, Fossen T I. Formation control of underactuated surface vessels using the Null-Space-Based behavioral control. In: Proceedings of IEEE/RSJ International Conference on Intelligent Robots and Systems, Beijing, 2006. 5942–5947

12 Ren W. Consensus strategies for cooperative control of vehicle formations. IET Control Theory Appl, 2007, 1: 505–512

13 Ren W, Sorensen N. Distributed coordination architecture for multi-robot formation control. Robot Auton Syst, 2008, 56: 324–333

14 Cao Y C, Ren W. Distributed formation control for fractional-order systems: dynamic interaction and absolute/relative damping. Syst Control Lett, 2010, 59: 233–240

15 Xiao F, Wang L, Chen J, et al. Finite-time formation control for multi-agent systems. Automatica, 2009, 45: 2605–2611

16 Hong Y G, Hu J P, Gao L X. Tracking control for multi-agent consensus with an active leader and variable topology. Automatica, 2006, 42: 1177–1182

17 Hu G Q. Robust consensus tracking of a class of second-order multi-agent dynamic systems. Syst Control Lett, 2012, 61: 134–142

18 Chen W S, Li X B, Jiao L C. Quantized consensus of second-order continuous-time multi-agent systems with a directed topology via sampled data. Automatica, 2013, 49: 2236–2242

19 Zhang H W, Lewis F L. Adaptive cooperative tracking control of higher-order nonlinear systems with unknown dynamics. Automatica, 2012, 48: 1432–1439

20 Cui R X, Ren B B, Ge S S. Synchronised tracking control of multi-agent system with high-order dynamics. IET Control Theory Appl, 2011, 6: 603–614

21 Chen W S, Li X B. Observer-based consensus of second-order multi-agent systems with fixed and stochastically switching topology via sampled data. Int J Robust Nonlin Control, 2014, 24: 567–584

22 Wang X L, Hong Y G, Huang J, et al. A distributed control approach to a robust output regulation problem for multi-agent linear systems. IEEE Trans Automatic Control, 2010, 55: 2891–2895

23 Hong Y G, Wang, X L, Jiang Z P. Distributed output regulation of leader-follower multi-agent systems. Int J Robust Nonlin Control, 2013, 23: 48–66

24 Li Z K, Duan Z S, Chen G R, et al. Consensus of multiagent systems and synchronization of complex networks: a unified viewpoint. IEEE Trans Circ Syst, 2010, 57: 213–224

25 Wen G H, Duan Z S, Yu W W, et al. Consensus in multi-agent systems with communication constraints. Int J Robust Nonlin Control, 2012, 22: 170–182

26 Zhang H W, Lewis F L, Das A. Optimal design for synchronization of cooperative systems: state feedback, observer and output feedback. IEEE Trans Autom Control, 2011, 56: 1948–1952

27 Zhang H W, Lewis F L, Qu Z H. Lyapunov, adaptive, and optimal design techniques for cooperative systems on directed communication graphs. IEEE Trans Ind Electron, 2012, 59: 3026–3041

28 Li Z K, Liu X D, Ren W, et al. Distributed tracking control for linear multi-agent systems with a leader of bounded unknown input. IEEE Trans Autom Control, 2012, 58: 518–523

29 Wen G H, Duan Z S, Chen G R, et al. Consensus tracking of multi-agent systems with lipschitz-type node dynamics and switching topologies. IEEE Trans Circ Syst I: Regular Papers, 2014, 61: 499–511

30 Chen W S, Li X B, Ren W, et al. Adaptive consensus of multi-agent systems with an unknown control directions based on a novel nussbaum-type function. IEEE Trans Autom Control, 2014, 59: 1887–1892

31 Li Z K, Duan Z S, Lewis F L. Distributed robust consensus control of multi-agent systems with heterogeneous matching uncertainties. Automatica, 2014, 50: 883–889

32 Peng Z H, Wang D, Zhang H W, et al. Distributed neural network control for adaptive synchronization of uncertain dynamical multiagent systems. IEEE Trans Neural Netw Learn Syst, 2014, 25: 1508–1519

33 Du H B, Li S H. Attitude synchronization control for a group of flexible spacecraft. Automatica, 2014, 50: 646–651

34 Liu T F, Jiang Z P. Distributed formation control of nonholonomic mobile robots without global position measurements. Automatica, 2013, 49: 592–600

35 Cui R X, Yan W S, Xu D M. Synchronization of multiple autonomous underwater vehicles without velocity measurements. Sci China Inf Sci, 2012, 55: 1693–1703

36 Krstić M, Kokotovic P V, Kanellakopoulos I. Nonlinear and Adaptive Control Design. New York: John Wiley & Sons, 1995

37 Li J H, Lee P M, Jun B H, et al. Point-to-point navigation of underactuated ships. Automatica, 2008, 44: 3201–3205

38 Tee K P, Ge S S. Control of fully actuated ocean surface vessels using a class of feedforward approximators. IEEE Trans Control Syst Tech, 2006, 14: 750–756

39 Chen M, Ge S S, How B V E, et al. Robust adaptive position mooring control for marine vessels. IEEE Trans Control Syst Tech, 2013, 21: 395–409

40 How B V E, Ge S S, Choo Y S. Dynamic load positioning for subsea installation via adaptive neural control. IEEE J Ocean Eng, 2013, 35: 366–375

41 Dai S L, Wang C, Luo F. Identification and learning control of ocean surface ship using neural networks. IEEE Trans Ind Inf, 2012, 8: 801–810

42 Skjetne R, Fossen T I, Kokotovic P V. Adaptive maneuvering, with experiments, for a model ship in a marine control laboratory. Automatica, 2005, 41: 289–298

43 Swaroop D, Hedrick J K, Yip P P, et al. Dynamic surface control for a class of nonlinear systems. IEEE Trans Autom

Control, 2000, 45: 1893–1899
44 Wang D, Huang, J. Neural network-based adaptive dynamic surface control for a class of uncertain nonlinear systems in strict-feedback form. IEEE Trans Neural Netw, 2005, 6: 195–202
45 Wang D. Neural network-based adaptive dynamic surface control of uncertain nonlinear pure-feedback systems. Int J Robust Nonlin Control, 2011, 21: 527–541
46 Li T S, Wang D, Feng G, et al. A DSC approach to robust adaptive NN tracking control for strict-feedback nonlinear systems. IEEE Trans Syst Man Cybernetics, Part B: Cybernetics, 2010, 40: 915–927
47 Tong S C, Li Y M, Feng G, et al. Observer-based adaptive fuzzy backstepping dynamic surface control for a class of MIMO nonlinear systems. IEEE Trans Syst Man Cybernetics, Part B: Cybernetics, 2011, 41: 1124–1135
48 Zhang T P, Ge S S. Adaptive dynamic surface control of nonlinear systems with unknown dead zone in pure feedback form. Automatica, 2008, 44: 1895–1903
49 Wang M, Liu X, Shi P. Adaptive neural control of pure-feedback nonlinear time-delay systems via dynamic surface technqiue. IEEE Trans Syst Man Cybernetics, Part B: Cybernetics, 2011, 41: 1681–1692
50 Xu B, Shi Z K, Yang C G, et al. Composite neural dynamic surface control of a class of uncertain nonlinear systems in strict-feedback form. IEEE Trans Cybernetics, 2014, 44: 2626–2660
51 Yoo S J. Distributed consensus tracking for multiple uncertain nonlinear strict-feedback systems under a directed graph. IEEE Trans Neural Netw Learn Syst, 2013, 24: 666–672
52 Cao C Y, Hovakimyan N. Novel L_1 neural network adaptive control architecture with guaranteed transient performance. IEEE Trans Neural Netw, 2007, 18: 1160–1171
53 Nguyen N T, Ishihara A K. Robust adaptive optimal control modification with large adaptive gain. In: American Control Conference, St Louis, 2009. 2581–2586
54 Yucelen T, Haddad W M. Low-frequency learning and fast adaptation in model reference adaptive control. IEEE Trans Autom Control, 2013, 58: 1080–1085
55 Fossen T I. Marine Control System, Guidance, Navigation and Control of Ships, Rigs and Underwater Vehicles. Trondheim, Norway, Marine Cyernetics, 2002
56 Franceschelli M, Gasparri A. On agreement problems with gossip algorithms in absence of common reference frames. In: International Conference on Robotics and Automation, Anchorage, 2010. 4481–4486
57 Chen M, Chen W H, Wu Q X. Adaptive fuzzy tracking control for a class of uncertain MIMO nonlinear systems using disturbance observer. Sci China Inf Sci, 2014, 57: 012207
58 Tong S C, Huo B Y, Li Y M. Observer-based adaptive decentralized fuzzy fault-tolerant control of nonlinear large-scale systems with actuator failures. IEEE Trans Fuzzy Syst, 2014, 22: 1–15
59 Khalil H K. Nonlinear Systems. Upper Saddle River: Prentice Hall, 2002
60 Stepanyan V, Krishnakumary K, Nguyenz N, et al. Stability and performance metrics for adaptive flight control. In: AIAA Guidance, Navigation, and Control Conference, Chicago, 2009. 1–19